

SPACE APPLICATIONS CENTRE
AHMEDABAD 380015
DOCUMENT CONTROL SHEET

Reference No.	SAC/EPESA/AMHTDG/HTDD/ATBD-01
Publication Date	19 March 2021
Title and Subtitle	Aerosol Optical Depth (AOD) Retrieval from Ocean Colour Monitor (OCM-2) onboard OceanSat-2
Type of Report	Algorithm Theoretical Basis Document (ATBD) (version-1.1)
No. of Pages	29
No. of Figures	10
Authors	Manoj K. Mishra
Originating Unit	Space Applications Centre, Ahmedabad.
Abstract	<p>This Algorithm Theoretical Basis Document (ATBD) describes the algorithm used to retrieve the Aerosol Optical Depth (AOD) for the OCM-2 instrument onboard OceanSat-2 a polar-orbiting platform.</p> <p>Specifically, this document identifies the sources of input data, both OCM-2 data and non-OCM-2 data, required for retrieval; provides the physical theory and mathematical background underlying the use of this information in the retrievals; includes implementation details; and describes assumptions and limitations of the proposed algorithm.</p>
Keywords	Aerosol optical depth, Fine mode fraction, Transmittance, Path radiance, Spectral response function.
Security Classification	Restricted
Distribution Statement	Limited to TEC committee members only.

Summary

Existing aerosol algorithms providing aerosol information over land take advantage of measurement in narrow bands falling in the wide spectral range from 0.4 to 2.5 μm or of polarization/multi-angle viewing capabilities or both. Most of the ISRO's space-borne sensors only partially fulfil the mentioned capabilities. As far as the requirement of narrow multiple channels in the visible region, and radiometric quality of the measurement is concerned, Ocean Colour Monitor (OCM-2) on-board OceanSat-2 seems to be a good choice, however, spectral coverage in OCM-2 is only up to 0.865 μm , which omitted the idea of aerosol remote sensing over land with existing algorithm. For this reason, to date OCM-2 was limited to ocean colour applications only.

This Algorithm Theoretical Basis Document (ATBD) describes a novel algorithm for remote sensing of aerosol over land using spectral reflectance observed by OCM-2. The algorithm retrieves the aerosol optical depth (AOD) as the primary product and fine mode fraction as a proxy for the size distribution (can be associated with anthropogenic sources) of the undisturbed aerosol column over most of the Indian landmass. The unique characteristic of OCM-2 is the presence of two narrow blue channels (0.44 and 0.49 μm), which is taken as an advantage in this algorithm for the resolution of aerosol type while optical depth inversion. The presence of two blue channels also allows full use of red and near-infrared (NIR) channels for surface characterization without any assumption on the transparency of aerosol in red and NIR bands. These two facts make this algorithm different from existing ones and also make aerosol remote sensing possible with OCM-2 sensor which does not have measurement capabilities beyond NIR like MODIS, VIIRS, and GOES-R, and do not have multi-viewings like MISR and PARASOL. The high brightness combined with spatial homogeneity of clouds in visible channels allows reasonably good cloud rejection while aerosol estimation. Co-located sun photometer validation is provided for the aerosol product.

The prime objectives for developing this aerosol product are to cater main input for air-quality, radiative budget, and climate applications, especially over Indian landmass. The high spatial resolution of 700 meters makes this product unique among globally available aerosol products. Apart from these, it will open the door for the utilization of OCM-2 data for other land applications also. Since OCM-2 in local area coverage mode have 2-day repetivity, the temporal resolution of OCM-2 AOD is two days, with an exception for the overlap region where daily retrievals are possible.

Contents

List Figures

List of Tables

List of Acronyms and Symbols

- 1.0 Algorithm Configuration Information
 - 1.1 Algorithm Name
 - 1.2 Algorithm Identifier
 - 1.3 Algorithm Specification
- 2.0 Introduction
 - 2.1 Overview and background
 - 2.2 Objectives
- 3.0 Inputs
 - 3.1 Static Data
 - 3.2 Image and pre-processing data (Dynamic)
 - 3.3 Other Auxiliary data and Model Inputs
- 4.0 Algorithm Functional Specifications
 - 4.1 Overview
 - 4.2 Instrument Characteristics
 - 4.3 Theoretical background
 - 4.3.1 Gas absorption
 - 4.3.2 Cloud and inland water masking
 - 4.3.3 Physical basis and model for surface characterization
 - 4.3.4 Radiative transfer calculations
 - 4.3.5 Aerosol inversion
 - 4.4 Flowchart
 - 4.5 Operational Implementation
- 5.0 Outputs
 - 5.1 Format of the output and the domain
- 6.0 Validation
 - 6.1 Data required
 - 6.2 Methods of validation
 - 6.2.1 AERONET data for validation
 - 6.2.2 Handheld sun photometer validation
 - 6.2.3 Satellite-based Inter-comparisons
 - 6.3 Provisional validation
 - 6.3.1 Derived AOD maps
 - 6.3.2 Validation results with AERONET data
- 7.0 Technical issues (Limitations etc.)
- 8.0 Future scope
- 9.0 Discussion
- 10.0 References

List of Figures

Figure 1. Spectral responses functions of Ocean Colour Monitor bands.

Figure 2. Local area coverage mode of Ocean Colour Monitor on-board OceanSat-2.

Figure 3. Atmospheric transmittance due to gas absorption for different values of water vapour and the standard value of oxygen (tropical atmosphere). Solar zenith assumed is 45 degrees and nadir viewing geometry.

Figure 4. Scatter plot for modelled surface reflectance in band-3 and band-6 versus surface reflectance obtained by atmospheric correction using in-situ data.

Figure 5. The overall workflow of the algorithm.

Figure 6. AOD map on 2 November 2016. High resolution (700m) of OCM-2 AOD enables one to capture high AOD/dust plume due to dust transportation from dust storms, which originated within India and in neighboring countries (e.g., Pakistan-Afghanistan border as shown).

Figure 7. High resolution (700m) from OCM-2 AOD enables one to capture high AOD/smoke plumes due to forest fires in North-East India and the neighboring countries.

Figure 8. (a) AOD map over eastern Indo-Gangetic plain (IGP) and central India on 15 January 2021. A very thick layer of aerosol (heavy air pollution) over IGP is observed. (b) Fine mode fraction map shows high fine aerosols in the entire IGP while relatively coarser sized particles in central India. (d) AERONET size distribution at Bholu station showing the dominance of fine mode aerosol.

Figure 9. Validation results of the OCM-2 AOD using AERONET in-situ AOD at different stations.

Figure 10. Drastic improvement in OCM-2 derived NDVI after correction for aerosol is apparent in the images shown.

List of Tables

Table 1. Summary of the OCM-2 aerosol optical depth (AOD) product

Table 2. Specification of Ocean Colour Monitor on-board OceanSat-2.

Table 3. Performance parameters of Ocean Colour Monitor on-board OceanSat-2.

Table 4. The coefficient that relates ozone optical thickness with concentration.

Table 5. Water vapour transmittance for OCM-2 band-8 centered at 865 nm at the solar zenith of 45 degrees and nadir viewing geometry.

List of Acronyms and Symbols

AOD	Aerosol Optical Depth
AWIFS	Advanced Wide Field Sensor
ATBD	Algorithm Theoretical Basis Document
AERONET	AERosol RObotic NETwork
DEM	Digital Elevation Model
EE	Error Envelope
FAOD	Fine mode Aerosol Optical Depth
FMF	Fine Mode Fraction
GAC	Global Area Coverage
HDF	Hierarchical Data Format
ISRO	Indian Space Research Organization
INSAT	Indian National Satellite
IRS	Indian Remote sensing Satellite
IGFOV	Instantaneous Geometric Field of View
IGP	Indo Gangetic Plain
LAC	Local Area Coverage
LUT	Look up Tables
LAADS DAAC	Level-1 and Atmosphere Archive & Distribution System Distributed Active Archive Center
L1B	Level-1 B
MODIS	Moderate Resolution Imaging Spectroradiometer
MISR	Multi-angle imaging spectroradiometer
NASA	National Aeronautics and Space Administration
NIR	Near Infrared
NDVI	Normalized Differential Vegetation Index
$Ne\Delta\rho$	Noise equivalent Reflectance
OCM	Ocean Colour Monitor
PARASOL	Polarization & Anisotropy of Reflectances for Atmospheric Sciences coupled with Observations from a Lidar
RT	Radiative Transfer
rmse	Root Mean Square Error
SRF	Spectral Response Function
SAC	Space Applications Center
SWIR	Short Wave Infrared
SNR	Signal to Noise Ratio
TOA	Top of the Atmosphere
TOMS	Total Ozone Mapping Spectrometer
VNIR	Visible to Near Infrared
VIIRS	Visible Infrared Imaging Radiometer Suite
VEDAS	Visualization of Earth observation Data and Archival System
O_3	Oxygen
H_2O	Water Vapour
O_2	Oxygen

R^2	Coefficient of determination
S	Slope of regression line
I	intercept of regression line
N	Number of data points
$\tau_{Rayleigh}$	Rayleigh or Molecular optical depth
τ	AOD or Aerosol optical depth
λ	Wavelength
λ_c	Central wavelength of a spectral band
K_{ext}	Extinction coefficient
z	Altitude
τ_{oz}	Ozone optical depth
K_{oz}	Ozone extinction coefficient
T_g	Gas transmittance
T_{oz}	Ozone transmittance
T_{H2O}	Water Vapour transmittance
θ	Sensor zenith
θ_0	Solar zenith
$\sigma_{\lambda,3 \times 3}$	Standard deviation of reflectance in a 3 x 3 pixel window
$NDVI$	Normalized Differential Vegetation Index
L_B	Band Radiance
L_{sat}	Saturation Radiance
$\rho_{\lambda}^{At.corr}$	Atmospherically corrected reflectance
ρ_{blue}^{sur}	Surface reflectance
ρ_{λ}^{TOA}	Top of the atmosphere reflectance
S_{λ}	Spherical albedo
ρ_{λ}^{RA}	Path reflectance
Ω_0	Sensor angles
Ω	Solar angles
E_0	Extraterrestrial irradiance
P	Phase scattering function
μ	Cosine of sensor zenith
μ_0	Cosine of solar zenith
ω_0	Single scattering albedo
I	Intensity
$n(r)$	Particle size distribution
ρ_{λ}^*	Modelled satellite level radiance

Aerosol Optical Depth (AOD) Retrieval from Ocean Colour Monitor (OCM-2) onboard OceanSat-2

1.0 Algorithm Configuration Information

1.1 Algorithm Name

OCM-2 Land Aerosol Optical Depth (AOD)

1.2 Algorithm Identifier

O2_*_AER_NDV

1.3 Algorithm Specification

Version	Date	Prepared by	Description
1.0	16 March 2021	Manoj K Mishra	OCM-2 AOD Baseline Document
1.1	25 March 2021	Manoj K Mishra	OCM-2 AOD Baseline Document

2.0 Introduction

2.1 Overview and background

Aerosols play an important role in numerous aspects of human life. Aerosols have largescale effects, such as their impact on climate by redistributing solar radiation (IPCC 2007; Charlson et al. 1991; Haywood et al. 1999) and interacting with clouds (Platnick and Twomey 1994; Kaufman et al. 2002). Aerosol information is also critical for atmospheric correction algorithms for multi-spectral satellite sensors and military operations. The climate effects of atmospheric aerosols may be comparable to carbon dioxide greenhouse effects, but with opposite signs and larger uncertainty (Hansen and Lacis, 1990). Aerosols have a significant impact on human life beyond the climate element. When in the lower troposphere aerosols cause poor air quality, reduction of visibility, and public health hazards. Satellite remote sensing provides a means to derive aerosol distribution at global and regional scales.

This Algorithm Theoretical Basis Document (ATBD) describes the algorithm used to retrieve the Aerosol Optical Depth (AOD) for the OCM-2 instrument onboard OceanSat-2 a polar-orbiting platform. The output product description is summarized in Table 1.

Specifically, this document identifies the sources of input data, both OCM-2 data and non- OCM-2 data, required for retrieval; provides the physical theory and mathematical background underlying the use of this information in the retrievals; includes implementation details; describes assumptions and limitations of the proposed approach.

Table 1. Summary of the OCM-2 aerosol optical depth (AOD) product

Parameter Name	Units	Horizontal Cell Size	Comments
Aerosol Optical depth @ 550nm	Dimensionless	700 meters over land.	Retrieved for all pixels except cloudy and saturated pixels.
Fine Mode Fraction	Dimensionless	700 meters over land.	Retrieved for all pixels except cloudy and saturated pixels.

2.2 Objectives

The primary objective of this algorithm is to calculate the aerosol optical depth, proportional to the total aerosol loading of the ambient aerosol, over land for the Indian region using OCM-2 data. The

secondary objective is to derive fine-mode fraction which is a proxy information about the particle size distribution and can be associated with anthropogenic sources of aerosols. The overall objectives of the aerosol retrieval are:

- To determine the aerosol optical thickness, at 550 nm and 700-meter spatial resolution over land within an uncertainty of 20%.
- To derive fine mode fraction as a qualitative indicator of anthropogenic pollution sources.

As clouds block the surface reflectance, the aerosol optical depth cannot be found for cloudy pixels therefore optical thickness retrievals apply only under clear and daytime conditions.

3.0 Inputs

3.1 Static Data

Input Name	Resolution	Units	Source
Digital elevation model (DEM)	1.0 km	meters	(GLOBE) Digital Elevation Model, Version 1.0, NOAA, (Hastings et al., 1999)
Spectral response function (SRF)	1.0 nanometres	dimensionless	SEDA/SAC/ISRO

3.2 Image and preprocessing data (Dynamic)

Input Name	Resolution	Quantization	Units	Source
OCM-2 radiometrically corrected TOA radiance in channels centred at 443, 490, 550, 620 and 865 nm	360 x 250 meters	12 bit	mW/cm ² /nm/sr	HDF L1 B data file (NRSC)
Sun-sensor geometry	pixel	-	degree	HDF L1 B data file (NRSC)
Latitude/Longitude	pixel	-	^o N / ^o E	HDF L1 B data file (NRSC)

3.3 Other Auxiliary data and Model Inputs

Input Name	Resolution	Units	Source
Ozone	1.0 x 1.25 degree, Monthly	Dobson	TOMS, NASA (Richard et al., 1998)
Simulated TOA radiance	6 degree interval sun-sensor geometry angles	mW/cm ² /nm/sr	Pre-calculated from RT model
Fine mode aerosol type	1 degree	dimensionless	Levy et al., 2007 (based on in-situ data from AEROET)

4.0 Algorithm Functional Specifications

4.1 Overview

Aerosol retrievals from polar-orbiting satellite data, such as Moderate Resolution Imaging Spectroradiometer (MODIS) of NASA's, Aqua and Terra Satellites, Visible Infrared Imaging Radiometer Suite (VIIRS), Multi-angle Imaging SpectroRadiometer (MISR), PARASOL are the major sources of high-quality global estimates of AOD over land and oceans ([Kaufman et al., 1997](#); [Levy et al., 2007](#); [Hsu et al., 2004, 2006, 2013](#)). All of these sensors of foreign space agencies are equipped with the channels to measure radiances in several narrow visible, near Infrared (NIR) and short-wave infrared (SWIR) spectral bands. In addition to measuring un-polarized spectral radiances at a single scattering angle, some of these sensors such as MISR and PARASOL can also measure un-polarized as well as polarized radiances at several scattering angles, thus providing more scope to improve the accuracy of AOD retrieval as well as aerosol optical properties. Most of these sensors utilize the dark-target method over dark vegetated surfaces and the deep-blue method over bright surfaces to retrieve AOD products. Both of these methods require spectral radiance measurement in at least three visible channels (near 440,490, 620 nm) and two SWIR channels (1.24 & 2.12 μm) for aerosol retrieval in addition to channels required for masking unwanted target pixels.

As far as Indian satellites are concerned, none of the existing sensors fulfils the requirements of measurement in all channels especially the SWIR channels, which is crucial for aerosol retrieval. Most of the spaceborne optical imaging sensors onboard different Indian Remote Sensing (IRS) satellites such as OceanSat (1, 2 and upcoming 3), CARTOSAT (1, 2 and 3) and RESOURCESAT (1 and 2), etc. were designed for specific applications related to Earth surface (land and ocean) monitoring and mapping, as in various EOS missions, and were not designed to accommodate channels for aerosol studies. For this reason, the existing AOD retrieval techniques requiring SWIR and visible channels, in multiple wavelengths, cannot be used for Aerosol retrieval from any of the ISRO sensors' data. INSAT-3D/3DR is the only exception, where utilizing the advantage of fixed view geometry due to Geostationary platform, a basic AOD product using single visible channel data without the need of SWIR measurement is operationally generated and is available for public use, on the SAC/VEDAS site ([Mishra et al., 2018](#)). However, this method is not so efficient or accurate and is not suited to good accuracy aerosol retrieval, which limits its use to qualitative estimate purpose, and time-series change monitoring only.

The reason for less research work toward the development of aerosol retrieval algorithm for single-view visible to near-infrared (VNIR) sensor in past may be due to significant aerosol contamination in the entire VNIR spectral range that makes surface characterization a difficult problem. Moreover, since electromagnetic radiation of SWIR (2 μm) wavelength minimally interact

with aerosols therefore researchers found MODIS-like sensors more feasible for developing relatively simpler aerosol retrieval algorithm.

Thus, due to the impracticality of implementation of existing AOD retrieval methods to ISRO's operational satellites' data, routine accurate AOD retrieval could not be done. However, extremely poor air quality over Indian landmass, especially the urban centers, and the high priority requirement from Environment Ministries, for high resolution (sub kilometres) aerosol estimations to generate ground-level PM_{2.5}/PM₁₀ maps, using existing Indian satellite sensor's data, an urgent need was there to develop techniques for retrieving reliable and accurate aerosol information from the existing Indian satellite sensors. Recent research work at Space Applications Center, ISRO, provides a unique solution to this. The research has led to the development of a Novel Technique, which can retrieve AOD from Ocean Colour Monitor (OCM) data onboard IRS OceanSat-2 satellite, which was launched in 2009 and is still in-service. This Algorithm Theoretical Basis Document briefly describes this aerosol algorithm and the aerosol product of which **AOD@550 nm beta version** is currently operational at **VEDAS/SAC/ISRO air quality portal** (<https://vedas.sac.gov.in/vstatic/AQ/index.html>).

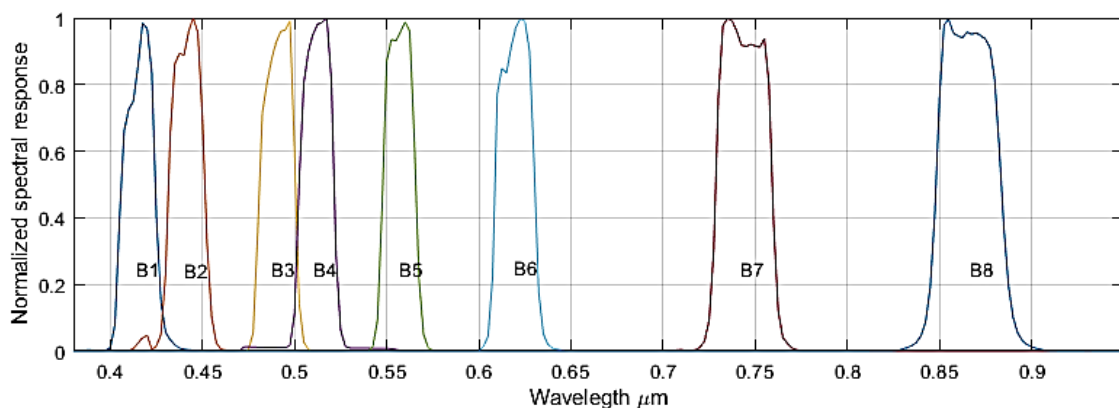


Figure 1. Spectral responses functions of Ocean Colour Monitor bands.

4.2 Instrument Characteristics

The OceanSat-2 was launched in 2009 and was placed in a near-circular sun-synchronous orbit, at an altitude of 720 Km, with an equatorial crossing time of around 1200 hrs. Ocean Colour Monitor is a VNIR sensor on-board OceanSat-2, which acquires top of the atmosphere radiance in 8 narrow spectral channels centered at wavelengths, 412, 443, 490, 510, 550, 620, 740, and 865 nm with high radiometric accuracy. Since 2010 (i.e., for the last 11 years) OCM-2 is continuously providing data over the ocean as well as on land and is still in service. Since OCM-2 is particularly designed for ocean colour studies, the ocean observation is planned at the local time of equator crossing

time of 1200 hours noon, the camera can be tilted up to $\pm 20^\circ$ in the along-track direction to avoid sun glint. Table 2 shows the salient characteristics of the OCM-2 sensor. Figure 1 shows the spectral responses of the channels. OCM-2 data is available in two spatial resolutions: Local Area Coverage (LAC) of 360 m and Global Area Coverage (GAC) of 1 km. To meet the objective of covering oceans around the Indian region, Real-Time LAC data is routinely received at the NRSC primary ground station. The area of coverage in LAC mode is shown in figure 2. Table 3 shows various performance parameters of OCM-2.

Table 2. Specification of Ocean Colour Monitor on-board OceanSat-2.

S.N.	Parameters	OCM-2 Specifications
1	IGFOV at nominal altitude (m)	360 x 250
2	Swath (km)	1420
3	No. of spectral bands	8
4	Spectral range (nm)	402-885
5	Spectral bands (nm)	B1: 402 – 422 nm B2: 433 – 453 nm B3: 480 – 500 nm B4: 500 – 520 nm B5: 545 –565 nm B6: 660 – 680 nm B7: 745 – 785 nm B8: 845 – 885 nm
6	Quantization bits	12
7	Tilt (to avoid sun glint)	$\pm 20^\circ$
8	Data acquisition modes	Local Area Coverage (LAC) – 360 m x 236 m Global Area Coverage (GAC) – 1 km x 1 km
9	Data formats	HDF

Table 3. Performance parameters of ocean colour monitor on-board OceanSat-2.

Band	Band center (λ_c), nm	SNR @ Ref. Radiance	Saturation radiance ($\text{mW}/\text{cm}^2/\text{sr}/\text{um}$)	Max ρ	$\text{Ne}\Delta\rho$ ($\times 10^{-3}$)	τ_{Rayleigh}
B1	412	356	70.2	1.29	3.00	0.210
B2	443	386	36.5	0.62	1.60	0.190
B3	490	380	29.6	0.48	1.30	0.150
B4	510	324	25.8	0.43	1.30	0.130
B5	550	312	21.2	0.36	1.20	0.090
B6	620	240	16.0	0.30	1.30	0.060
B7	740	286	1.9	0.05	0.17	0.030
B8	865	141	14.3	0.49	3.50	0.017

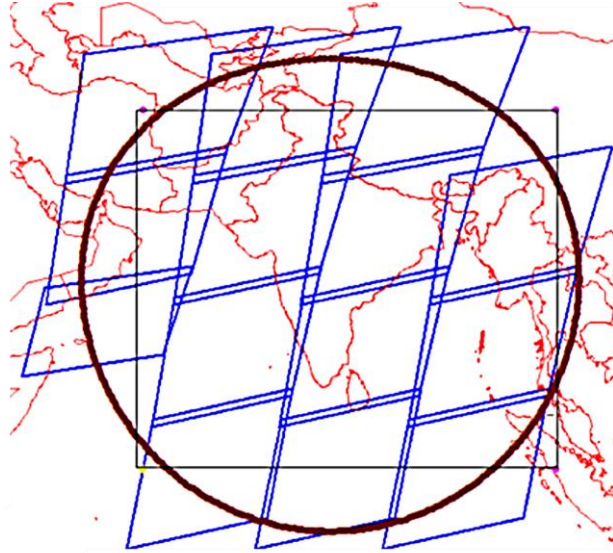


Figure 2. Local area coverage mode of Ocean Colour Monitor on-board OceanSat-2..

4.3 Theoretical background

AOD τ is the measure of aerosols distributed within the column of air from the ground instrument to the top of the atmosphere or from the space-borne sensor to the surface. AOD is the degree to which aerosol prevents the transmission of the light by absorption or scattering of light and is defined as the integrated extinction coefficient of light due to aerosol over a vertical atmospheric column of unit cross-section (mathematically represented by equation 1). Extinction coefficient K_{ext} is defined as the fractional depletion of radiance per unit length.

$$\tau = \int_0^l K_{ext}(z) dz \quad (1)$$

The following description is intended to provide the basic structure of the algorithm that can derive aerosol optical depth and fine mode fraction from OceanSat-2 OCM data, which acquires top of the atmosphere radiance in 8 narrow spectral channels centered at wavelengths, 412, 443, 490, 510, 550, 620, 740 and 865 nm with high radiometric accuracy. The overall workflow for the proposed algorithm/technique for aerosol retrieval using OCM-2 data is shown in section 4.4. It mainly involves four components:

- (a) Masking of the pixel for which retrieval is not possible (e.g., cloud, water, and saturated pixels),
- (b) The surface characterization in visible-channels,
- (c) Radiative transfer simulation, and
- (d) The aerosol inversion.

The aerosol retrieval algorithm described in this ATBD is novel/different from other existing aerosol retrieval algorithms such as dark-target or deep-blue in many ways that make it capable to derive aerosols from VNIR sensors. Following are the salient points of the algorithm:

- (a) The surface characterization in visible channels is shown to be possible by the use of near Infrared channel measurements, where the existing algorithm uses the SWIR channel over dark targets and reflectivity database over bright surfaces. Thus this algorithm avoids the necessity of SWIR measurement as well as doesn't require the pre-existence of a surface reflectivity database.
- (b) Different from the dark-target algorithm, the surface characterization strategy in this algorithm is not limited to vegetative surfaces but is also valid over moderately bright surfaces, which enables AOD retrieval over both moderately bright as well as dark surfaces.
- (c) Different from the dark-target, deep-blue algorithm and others where blue and red channels are used for aerosol inversion, in this algorithm aerosol inversion is based on two blue channels which allows more accurate selection of aerosol types and also increases the probability of retrieval over bright targets.

Apart from this many other differences such as red and NIR bands are not assumed transparent, simultaneous retrieval of aerosol and surface in NIR and red bands, etc., makes the current aerosol retrieval algorithm novel when compared to existing ones, though none of them are feasible for implementation with OCM-2 sensor.

4.3.1 Gas absorption

In addition to the aerosols and molecular scattering, certain atmospheric gases may also affect OCM-2 channels. In the VNIR region, primarily three atmospheric gas may absorb the incident solar radiation and upwelling radiation namely water vapour (H₂O), ozone (O₃), and oxygen (O₂). The expression for ozone optical thickness, $\tau_{oz}(\lambda)$ for OCM:

$$\tau_{oz}(\lambda) = K_{oz}(\lambda) DU \quad (1)$$

where, DU refer to total column ozone in Dobson unit and $K_{oz}(\lambda)$ is the extinction coefficient that relates optical thickness with concentration. Table 4 show the values of $K_{oz}(\lambda)$ for OCM-2 channels. From table 4 it can be seen that band-5 and band-6 centered at 550 and 620 nm, respectively are significantly affected by ozone absorption. The top of the atmosphere radiance is corrected by ozone transmittance. The relation for the ozone transmittance is:

$$T_{oz} = \exp[-\tau_{oz}(\lambda)\{(cos\theta)^{-1} + (cos\theta_0)^{-1}\}] \quad (2)$$

Since OCM-2 channels are selected in atmospheric windows, therefore, absorption due to water vapour and oxygen is expected to be insignificant. To verify this figure 3 shows the transmittance due to water vapour at different concentrations (2, 4, and 6 cm) and the standard value of oxygen for the tropical atmosphere. From figure 3, it is clear that that band 2, 3, 5 and 6 are completely free from the water vapour or oxygen absorption. Band 8 is also almost free from water vapour but with very little contamination, however. Table 5 shows the water vapour transmittance obtained after convolving the transmittance curve with band-8 spectral response function, where from it is verified that the contamination is not more than 1% even at high water vapour content of around 6 cm. There may be an error of about 1-2% if water vapour content is very high >6 cm but such conditions are rare and often gets masked as clouds.

Table 4. The coefficient that relates ozone optical thickness with concentration.

Band λ (nm)	412	443	490	510	550	620	740	865
$K_{oz}(\lambda) 10^{-4}$	0.008	0.039	0.249	0.384	0.989	0.856	0.139	0.034

Table 5. Water vapour transmittance for OCM-2 band-8 centered at 865 nm at the solar zenith of 45 degrees and nadir viewing geometry.

H ₂ O (cm)	0	2	4	6	8	10
$T_{H_2O} 10^{-4}$	1.0	0.995	0.990	0.987	0.983	0.980

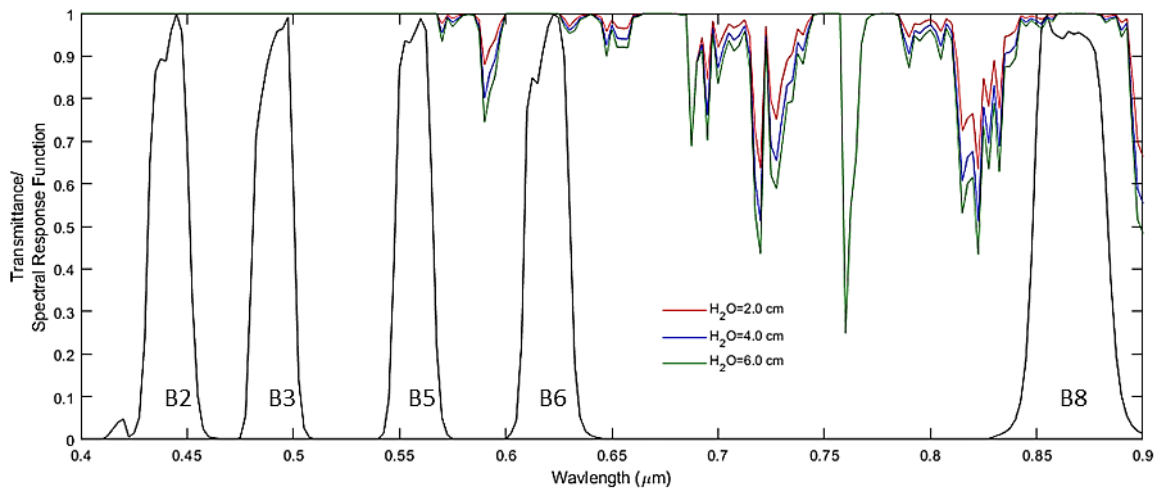


Figure 3. Atmospheric transmittance due to gas absorption for different values of water vapour and the standard value of oxygen (tropical atmosphere). Solar zenith assumed is 45 degrees and nadir viewing geometry.

4.3.2 Cloud and inland water masking

Masking clouds retaining heavy aerosol events unmasked is very challenging in any aerosol retrieval algorithm. In normal conditions, heavy/thick clouds can be distinguished and masked just by applying an appropriate threshold on visible channel measurements, however, thin clouds especially at cloud edges frequently create problems. An astringent threshold can be used to mask such pixels but it also masks heavy aerosol plumes. For this reason in the present algorithm, a visible channel threshold is used to mask thick clouds only. For masking scattered clouds, a spatial homogeneity test is performed by estimating the standard deviation over a running window of 3x3 pixels. An appropriate threshold is used to detect scattered cloudy pixels keeping the fact in mind that the land surface is more homogeneous than the scattered clouds. For cloud masking following 2 tests are performed:

(a) Visible channel (band-2) reflectance threshold test:

$$\rho_{443\text{ nm}} > 0.30 \quad \text{Pixel is considered cloudy.} \quad (3)$$

(b) Threshold test on the standard deviation of a running 3 x 3-pixel window of band-2 image.

$$\sigma_{443\text{ nm}, 3 \times 3} > 0.02 \quad \text{Center pixel is considered cloudy.} \quad (4)$$

The inland water mask is determined by computing the traditional NDVI like parameter (NDVI') for the 0.62 μm and the 0.865 μm channels.

$$NDVI' = \frac{\rho_{B8,TOA} - \rho_{B6,TOA}}{\rho_{B8,TOA} + \rho_{B6,TOA}} \quad (5)$$

If $NDVI' < 0.05$ then the pixel is considered water contaminated and is masked.

The test for pixel saturation is also performed using saturation radiance (L_{sat}) values for each band. If measured radiance (L_B) in any band satisfies the condition

$$L_B > L_{sat} \quad (6)$$

then the pixel is considered saturated and is masked.

Any pixel with solar zenith angle (θ_0) or sensor zenith angle (θ_0) above-given limits are also masked. The condition for the high zenith angle test is given by:

$$\theta_0 > 72^\circ \quad \text{or} \quad \theta > 84^\circ \quad (7)$$

4.3.3 Physical basis and model for surface characterization

The physical basis behind surface characterization in visible channels using NIR channels is based on the fact that over the vegetated surface, the surface reflectance in the blue spectral region is low due to absorption of solar radiation by chlorophyll while in the NIR region the surface reflectance becomes high due to specular reflection from the

leaves. Using this fact appropriate function of the form shown in equation 8 can be developed to characterize the surface reflectance in blue and red channels knowing the surface reflectance in NIR channels and an appropriate vegetation index. For the case of OCM-2 data, the vegetation index used is NDVI, blue and red, and NIR channels used are centered at 443 nm, 490 nm, 620 nm, and 865 nm.

$$\rho_{blue}^{sur} = f(\rho_{NIR}^{At.corr}, NDVI), \quad (8)$$

$$NDVI = \frac{\rho_{NIR}^{At.corr} - \rho_{red}^{At.corr}}{\rho_{NIR}^{At.corr} + \rho_{red}^{At.corr}} \quad (9)$$

$$\rho_{\lambda}^{At.corr} = \frac{\rho_{\lambda}^{TOA}(\Omega_0, \Omega) - T_g(\Omega_0, \Omega) \rho_{\lambda}^{RA}(\Omega_0, \Omega, \tau)}{T_g(\Omega_0, \Omega) T(\Omega_0, \tau) T(\Omega, \tau) + S_{\lambda}(\tau) [\rho_{\lambda}^{TOA}(\Omega_0, \Omega) - T_g(\Omega_0, \Omega) \rho_{\lambda}^{RA}(\Omega_0, \Omega, \tau)]} \quad (10)$$

For developing relation given in equation (8), around 1860 OCM-2 datasets (for the year 2017) were processed and corrected for aerosol and gas absorption at 22 AERONET stations (located in India, Pakistan, Nepal, Bangladesh, and Myanmar) using in-situ aerosol, water vapour, and ozone information. After cloud screening of both AERONET and OCM-2 data around 700 co-located data-points are selected for model development. Radiative transfer calculations were used to generate benchmark datasets of surface reflectance for each spectral channel. The performance of function developed to estimate band-3 and band-6 surface reflectance using NIR channel is shown in figure 3. From figure 3 it is seen that surface reflectance in band-3 can be estimated using both red as well as NIR bands and NDVI within root mean square error (rmse) of around 0.02. For lower surface reflectance the scatter is less while on bright surfaces the significant scatter is observed. In figure 4, the data point density is higher for low surface reflectance pixels, which in general true as natural targets are dark in blue wavelengths, therefore excluding bright surface the rmse will become significantly lower than 0.02. In a similar way, function to estimate surface reflectivity in band-2 using band-3 is also developed.

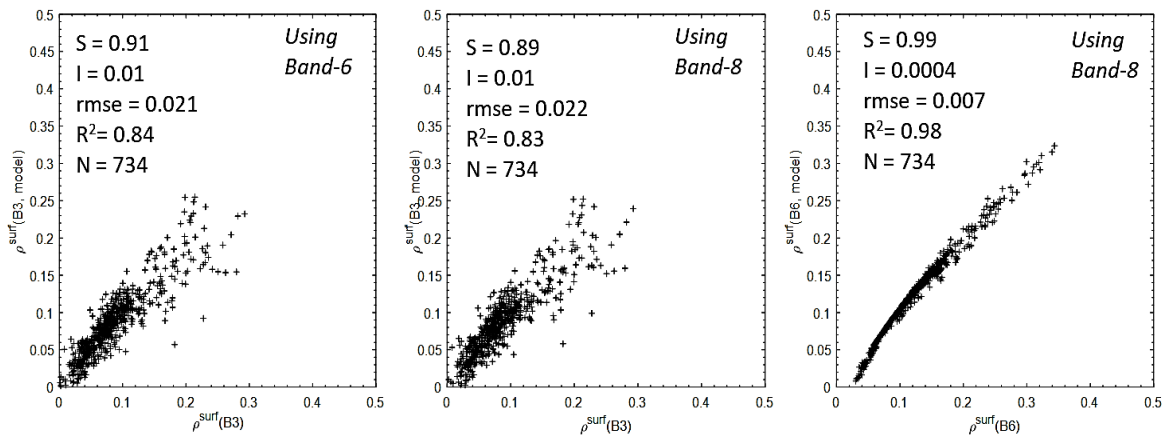


Figure 4. Scatter plot for modelled surface reflectance in band-3 and band-6 versus surface reflectance obtained by atmospheric correction using in-situ data.

4.3.4 Radiative transfer calculations

Radiative Transfer (RT) simulation is another important step towards aerosol retrieval in which the method of discrete ordinate is used to solve the RT equation (equation 11) for simulating various radiative quantities for different possible aerosol atmospheres and illumination-view geometries.

$$\mu \frac{dI(\tau, \Omega)}{d\tau} = I(\tau, \Omega) - \frac{\omega_0}{4\pi} \int_{4\pi} I(\tau, \Omega') P(\Omega, \Omega') d\Omega' - \frac{\omega_0}{4\pi} E_0 P(\Omega, -\Omega_0) \exp(-\frac{\tau}{\mu_0}). \quad (11)$$

Solving this equation, the top of the atmosphere radiance (L_{sat}^*) can be computed assuming tropical atmosphere in the range of 0.4-1.0 μm at the spectral resolution of 0.0025 μm , which are then convoluted to OCM-2 spectral response functions to simulate observations. The radiative scattering due to aerosols is simulated assuming 2 fine aerosol models defined as moderately and strongly absorbing aerosols, and 1 coarse aerosol model named dust aerosol model. The optical properties (extinction and scattering coefficients, single scattering albedo, phase function, and asymmetry factor) of the basic modes (accumulation and coarse modes) are computed from the Mie theory assuming multi-modal log-normal distribution defined by

$$n(r) = \sum_{i=1}^N \frac{f_i}{r \ln \sigma_i} \exp\left[\frac{\ln^2 r / r_{m,i}}{2 \ln^2 \sigma_i}\right], \quad (12)$$

where N is the number of modes, r is the particle radius, $r_{m,i}$ is the mean radius of mode i , σ_i is the width of mode i , and f_i is the number density of mode i . These parameters and the refractive index ($m_i = m_{i,real} + m_{i,img}$) for each mode used in Mie calculations are taken from [Levy et al., 2007](#). An exponential profile of AOD with a scaled height of 2 km is assumed. In the current version of the algorithm, to reduce the computational time of operational retrieval of AOD, RT simulation-based look-up-tables (LUTs) are generated and saved as the auxiliary database, which is used to calculate the ρ_{sat}^* as a function of solar zenith θ_o , sensor zenith θ , relative azimuth angle $\Delta\phi$, ρ_s and AOD (varied from 0-5). LUTs corresponding to AOD = 0, 0.25, 0.5, 0.75, 1.0, 2, 3.0, 5.0 for each spectral band are generated and saved. Each LUT contains calculated path reflectance for ten θ_o and θ values ranging from 0.0 to 72.0 with an interval of 6.0 degrees and for sixteen $\Delta\phi$ values ranging from 0.0 to 180.0 with an interval of 12 degrees. For RT simulation several ready-to-use codes are freely available, however, in the current version of the algorithm, the discrete ordinate method is used for which CDISORT code is customized as per the need.

4.3.5 Aerosol inversion

The radiance data for two blue channels (443 and 490 nm in the case of OCM-2) are then compared with modelled radiance. A maximum likelihood method is used to match the appropriate values of aerosol optical thickness at 550nm and mixing ratio to the measured radiance. For estimating the best solution, first AOD solutions using different aerosol models (represented by 12 values of fine mode fraction ranging from -0.1 to 1.1) is estimated by finding the perfect match between modelled and observed radiance in band-3 (490 nm), secondly among these best AOD solutions one is chosen as the final solution by comparing modelled and measured radiance in band-2 (443nm). The technique thus derived gives a procedure, which is performed on each cloud-free land pixel, giving one of the finest daily aerosol optical depth (AOD) at 550nm and fine mode fraction. Mathematically for each pixel, a set of AOD and fine mode fraction is found for which the equations (13) and (14) are satisfied.

$$\rho_{490}^* - \rho_{490}^{TOA} = 0, \quad (13)$$

$$\rho_{443}^* - \rho_{443}^{TOA} = \varepsilon_{min}. \quad (14)$$

Here ρ_{λ}^* and ρ_{λ}^{TOA} stands for satellite level modelled and measured signal (reflectance or radiance), respectively, for band centered at wavelength λ and ε_{min} stands for residual error. The satellite level modelled reflectance ρ_{sat}^* is estimated by linear mixing of satellite level modelled reflectance for fine mode and coarse mode aerosol models represented by symbols $\rho_{\lambda, fine}^*$ and $\rho_{\lambda, coarse}^*$, respectively, and weighted by fine mode fraction FMF . Mathematically it can be represented by the relation:

$$\rho_{\lambda}^* = FMF \rho_{\lambda, fine}^* + (1 - FMF) \rho_{\lambda, coarse}^*. \quad (15)$$

4.4 Flowchart

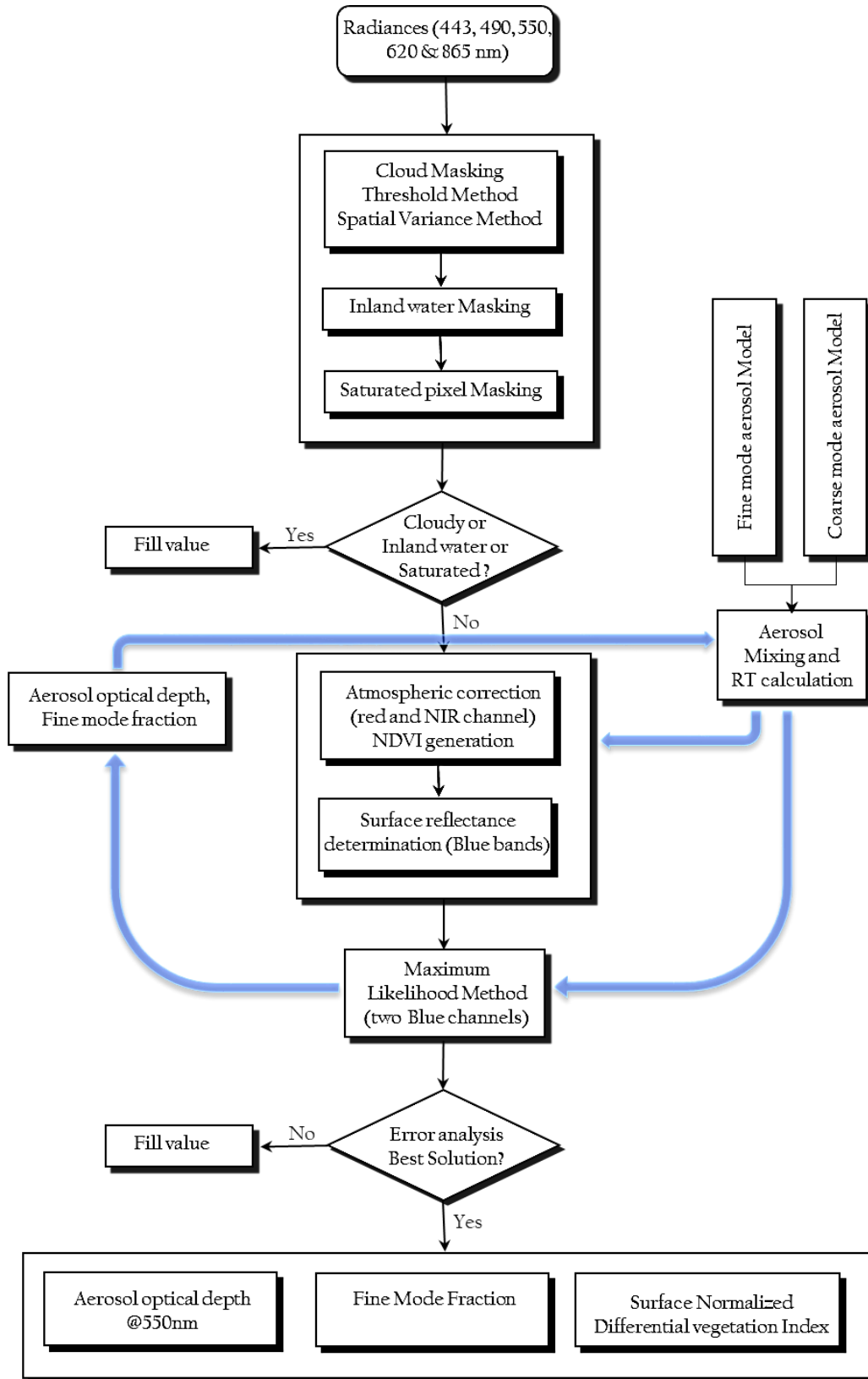


Figure 5. The overall workflow of the algorithm.

4.5 Operational Implementation

Step 1: Reading visible channel radiance, sun-sensor geometry, and geolocation data.

Step 2: Apply calibration coefficients to radiance data.

Step 2: Down-sampling of each spectral band radiance by 3 x 3 window averaging.

Step 3: Cloud masking, Saturation pixel masking, Inland water masking, Ocean masking.

Step 4: Ozone correction to each channel radiance.

Step 5: Surface characterization in blue channels.

Step 6: LUT Interpolation.

Step 7. Use LUTs for inversion of aerosol optical depth (AOD) and fine mode fraction.

Step 8: Repeat steps 4 to 8 for each unmasked pixel.

Step 9. Geo-referencing & resampling the output AOD and fine mode fraction at 0.7 km.

5.0 Outputs

Parameter	Unit	Min	Max	Accuracy	Resolution
Aerosol optical depth at 550 nm	Dimensionless	0	5	Uncertainty <20% (Targeted)	0.7 km
Fine mode fraction	Dimensionless	0	1	Qualitative indicator	0.7 km

5.1 Format of the output and the domain

Geocoded tiff data files for each path and row. Having 3 layers: AOD @550nm, Fine mode fraction, and aerosol corrected surface NDVI.

Domain: Local area coverage as shown in figure 2.

6.0 Validation

6.1 Data required

Parameter	Resolution	Accuracy	Source
AERONET spectral AOD data	In-situ point data	≤ 0.02	AERONET site in India & neighbouring countries
Spectral AOD using handheld sun-photometer	In-situ point data	≤ 0.02 .	Data collection campaigns will be organized
MODIS/VIIRS AOD product	0.1 x 0.1 degree	$\pm(0.05+0.2 \text{ AOD})$	LAADS DAAC - NASA

6.2 Methods of validation

6.2.1 AERONET data for validation

Ground-based observations can be made using AERONET (Holben et al., 1998), and any of the several miscellaneous techniques, including the diffuse/direct method and polarization measurements. AERONET (Aerosol Robotic Network) is a network of ground-based sun photometers established and maintained by Brent Holben of Code 923 of the NASA Goddard Space Flight Center and Tom Eck of Raytheon ITSS. The sun-photometers measure the spectral aerosol optical thickness and sky radiance. In India 4 AERONET sites namely Jaipur, Kanpur, Gandhi College, and Amity University Noida; in Bangladesh 2 sites namely Bhola and Dhaka University; in Pakistan Lahore and Karachi, and few sites in Nepal and Myanmar are providing systematic in-situ AOD measurements. Data from these sites will be used for validation of OCM-2 derived AODs after proper co-location in space and time.

For co-location of AERONET data with OCM-2 AOD retrievals, the in-situ AOD measurements will be averaged in a ± 30 minute window centered at the time of OCM-2 AOD retrievals. It is to be noted that different AERONET stations may have a different temporal resolution of the in-situ measurement, therefore, along with overall validation, the variation in validation results when using in-situ data at different temporal resolution will also be studied.

6.2.2 Handheld sun photometer validation

Many of the present satellite observations are augmented by special field campaigns to provide ground-truth data for the satellite-derived measurements. Ongoing and Past data from such campaigns will be used for validation.

6.2.3 Satellite-based Inter-comparisons

OCM-2 derived AOD may be validated by comparing them with aerosol optical depths derived by other satellite sensors, such as MODIS/VIIRS. The basic inter-comparison technique involves three steps: 1) Identification of locations where both sensors fly over at nearly the same time; 2) Extraction of data for storage in an inter-comparison archive; 3) Analysis of the differences between the measurements.

6.3 Provisional validation

6.3.1 Derived AOD maps

Figures 6, 7, and 8 display the ability of the developed aerosol product to capture different sources of aerosols such as small to large-scale forest fires, dust storms, and anthropogenic activities over different parts of India. Due to high-resolution data (figure 6) it is evident that

the spatial distribution of aerosol over megacities such as Delhi can be monitored using the OCM-2 AOD product. The availability of high-resolution spatial distribution of aerosol from space over megacities will play a major role in developing a product such as ground particulate matter (PM_{2.5} and PM₁₀) maps at a large scale, which will be helpful in monitoring of air-quality and developing mitigation techniques in metropolitan cities.

In figure 8, the AOD map, fine mode fraction map, and AOD histogram are shown for data acquired by OCM-2 over eastern Indo-Gangetic plain (IGP) and central India on 15 January 2021. The particle size distribution function from AERONET data at Bhola station, Bangladesh is also shown in figure 8 for the same date. A very thick layer of aerosol (heavy air pollution, AOD>1.0) over IGP is observed. The AERONET stations located at Dhaka University and Bhola, Bangladesh show very high AOD values of 1.5 and 1.25, respectively. OCM-2 AOD retrieval is consistent with ground observations. A fine mode fraction map shows high fine aerosols in the entire IGP, while relatively coarser-sized particles in central India are observed. It is well known that during winter's high anthropogenic pollution associated with the biomass/biofuel combustion process occurs over IGP giving rise to fine aerosols. The dominance of fine mode aerosol is also verified by size distribution observations at AERONET stations Dhaka University and Bhola.

6.3.2 Validation results with AERONET data

As described previously the retrieved products must look reasonable, and must be evaluated about ground-truth data. The test data includes the entire 2016 data i.e., almost around 1092 L1B datasets were processed to generate the aerosol product. Out of these 180 individual granules corresponding to path-9, row-13 (during the entire year of 2016) enclosing four AERONET stations namely Kanpur, Jaipur, Gual Pahari (India), and Karachi (Pakistan) are used for validation with ground truth. Among these, 3 stations, are interior urban centers and mainly affected by anthropogenic sources of aerosols. Over Karachi, being a coastal city, the aerosols are also affected by marine sources (sea salt) in addition to anthropogenic sources. The results are shown in figure 9. A very good correlation, of around 0.8 is observed. About 63% to 80% of AOD retrievals are within the error envelope (EE) of 20%. The results show that the proposed algorithm is highly sensitive towards aerosol retrieval using VNIR observation from the OCM-2 sensor. A slight deviation of the slope of the regression line may be due to several reasons but most probably it is due to calibration error, deviation of aerosol optical properties used for inversion, and/or due to uncertainty in surface characterization in the visible channel. These factors need to be improved in future versions.

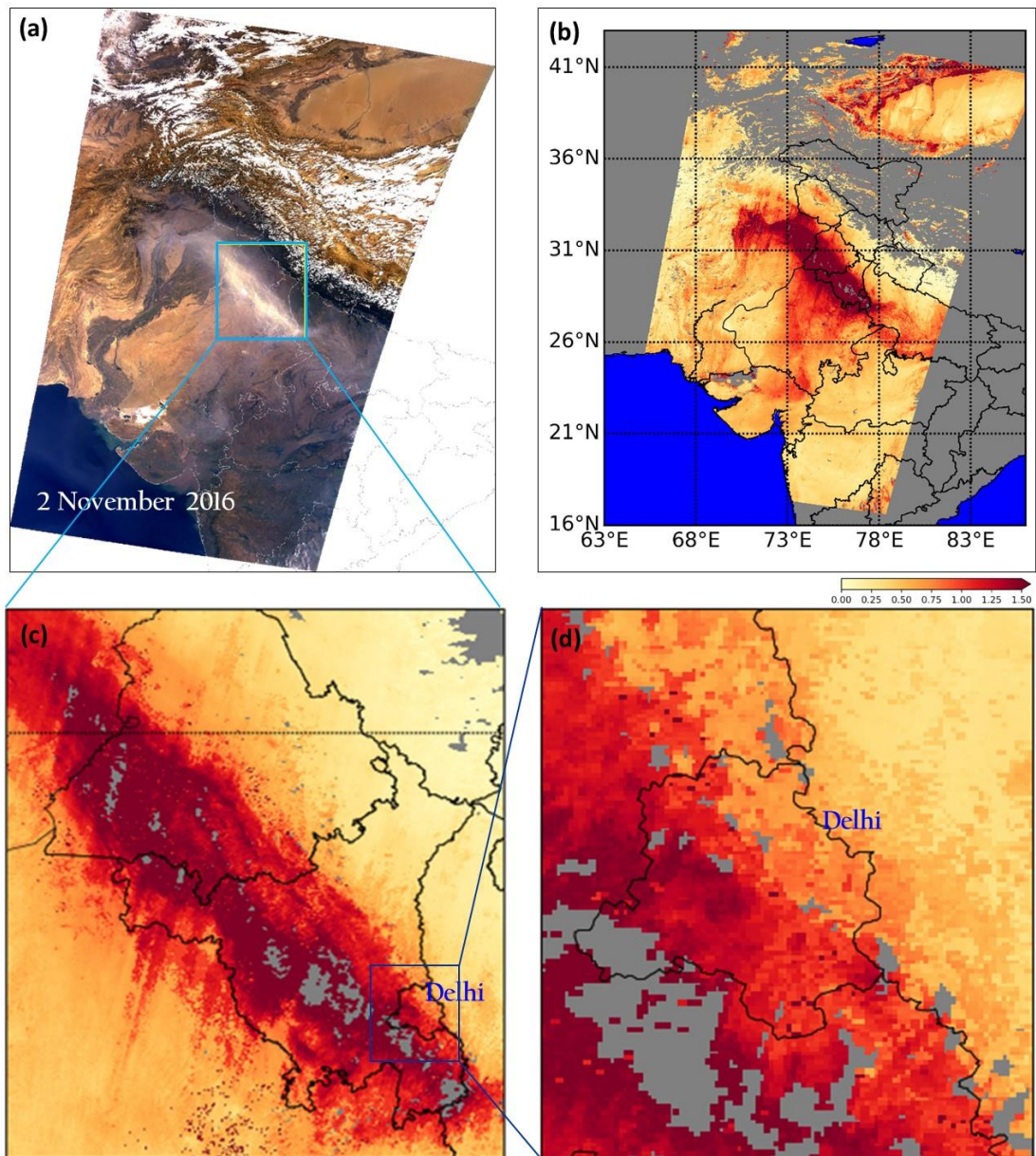


Figure 6. AOD map on 2 November 2016. High resolution (700m) of OCM-2 AOD enables one to capture high AOD/dust plume due to dust transportation from dust storms, which originated within India and in neighboring countries (e.g., Pakistan-Afghanistan border as shown).

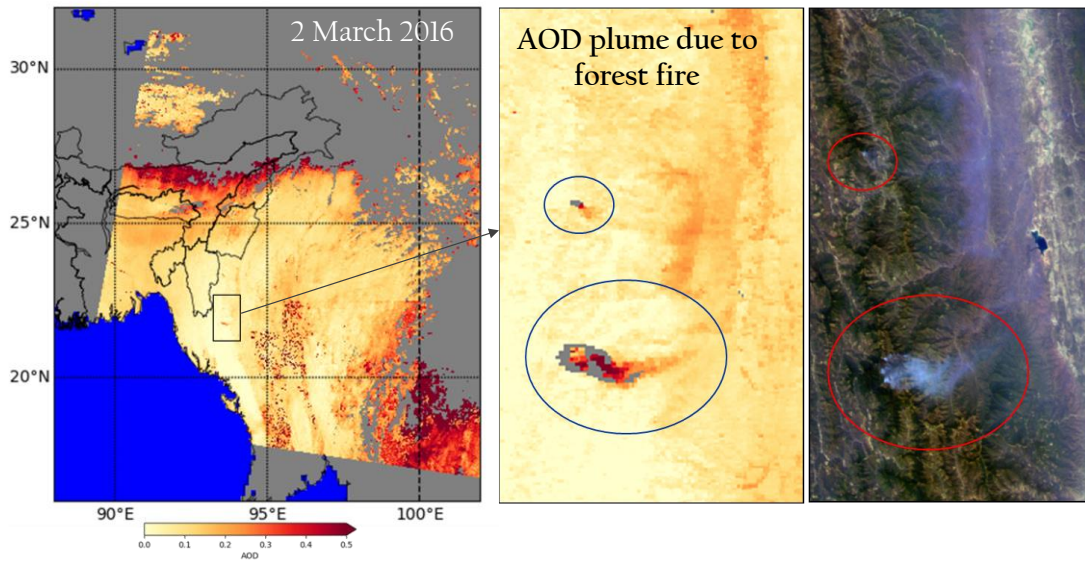


Figure 7. High resolution (700m) from OCM-2 AOD enables one to capture high AOD/smoke plumes due to forest fires in North-East India and the neighboring countries.

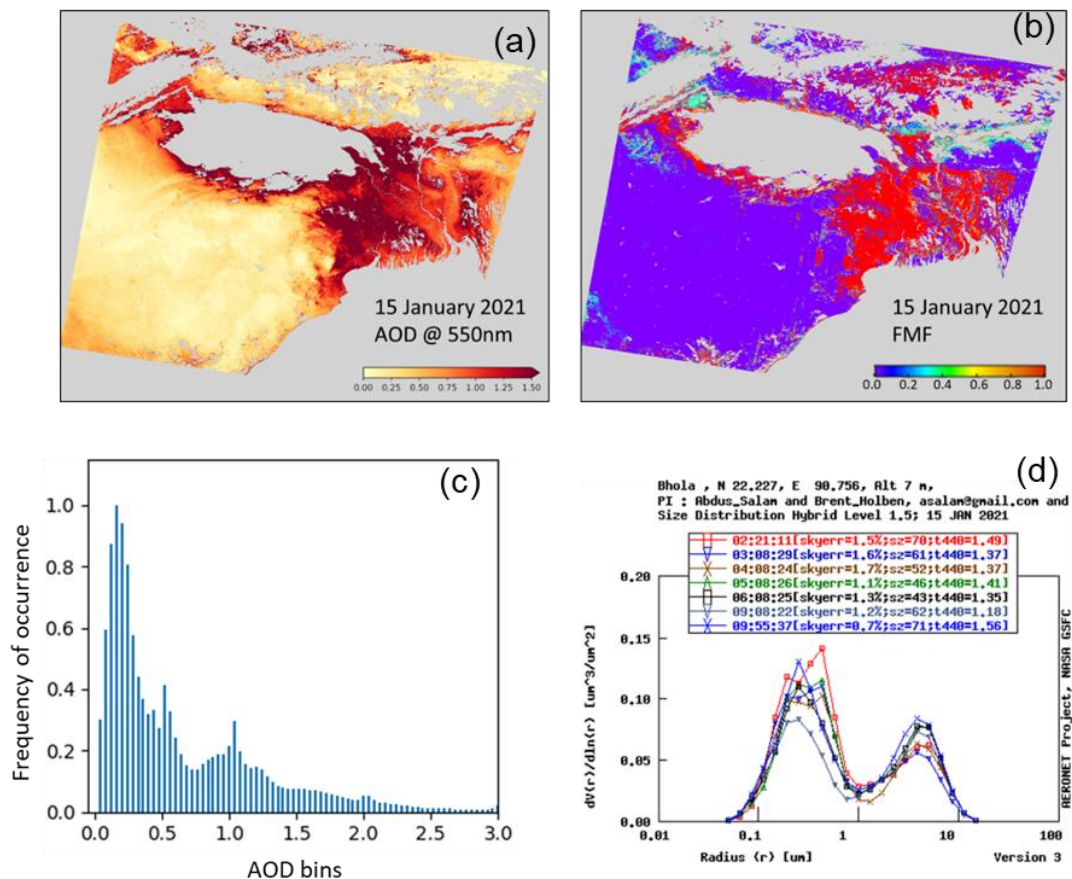


Figure 8. (a) AOD map over eastern Indo-Gangetic plain (IGP) and central India on 15 January 2021. A very thick layer of aerosol (heavy air pollution) over IGP is observed. (b) Fine mode fraction map shows high fine aerosols in the entire IGP while relatively coarser sized particles in central India. (d) AERONET size distribution at Bhola station showing the dominance of fine mode aerosol.

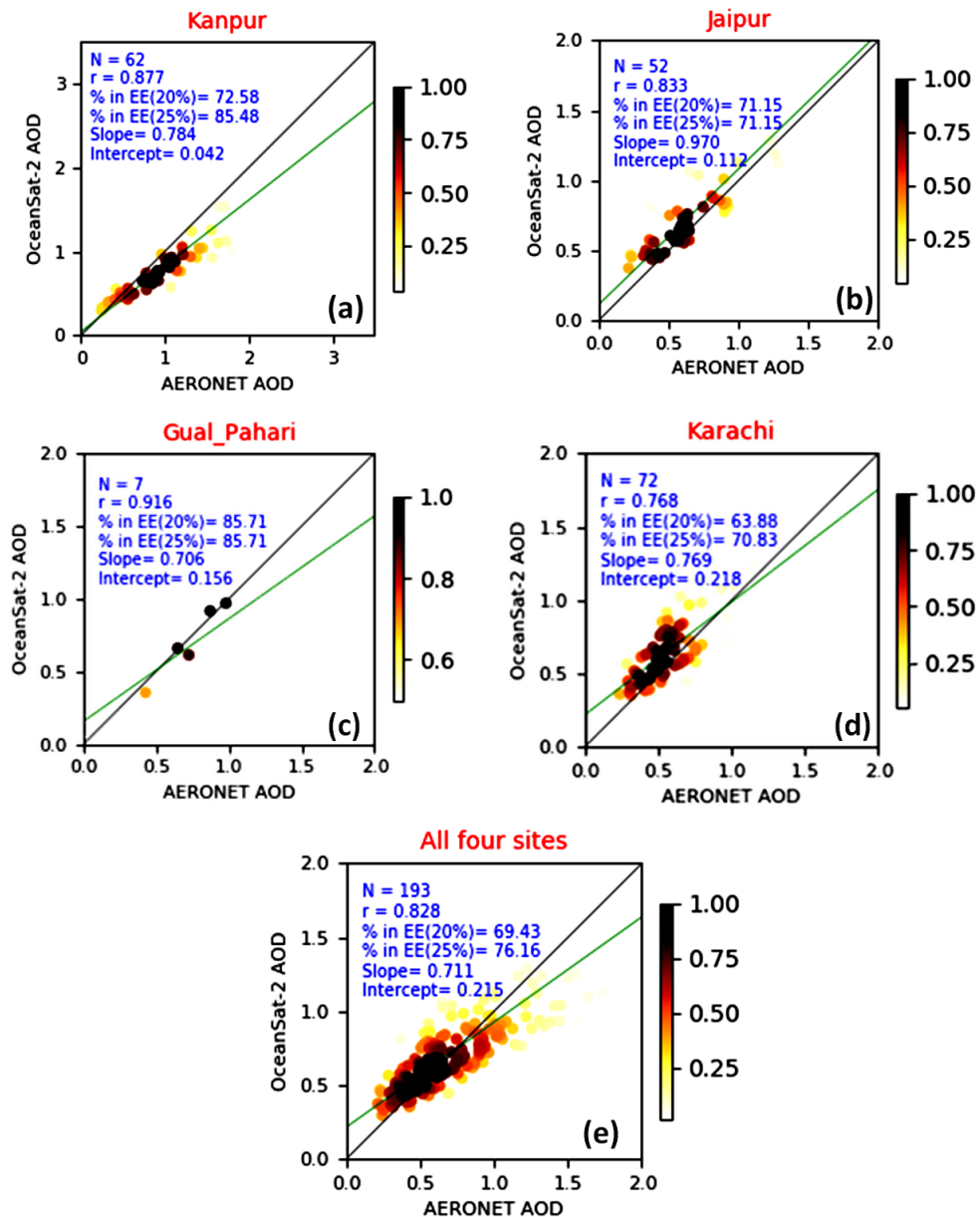


Figure 9. Validation results of the OCM-2 AOD using AERONET in-situ AOD at different stations.

7.0 Technical issues (Limitations etc.)

- The aerosol retrieval may fail at very bright surfaces due to physical limitations or due to the saturation of data. For very bright surfaces after a certain value of aerosol optical depth, the model radiance becomes highly inaccurate.
- In the current version of the algorithm, the fine mode fraction values are used at discrete levels therefore fine mode maps may show pixelated appearance.
- Validation of the fine mode fraction is difficult as no in-situ observations are available, however, in the future fine mode AOD (FAOD) may be correlated with AERONET inverted FAOD values.
- Using OCM-2 channels it is not possible to identify snowy pixels, therefore though snow pixels are expected to be masked as cloudy pixels due to high reflectance but still partially snow contaminated or less reflecting snow pixels may so unexpected AOD retrieved values. In

future versions, AWIFS based snow climatology can be used for the identification of snowy pixels.

- For AOD retrievals the OCM-2 radiance image is down-sampled by the average filter of 3 x 3-pixel size to improve the signal-to-noise ratio required for AOD retrieval. If retrieval is performed at the original resolution the uncertainty may reach above the targeted uncertainty of <20%.
- It is to be noted the aerosol retrieval is very sensitive to the radiance calibration as well as to surface reflectance. An error of 1% sensor measured reflectance or in surface reflectance may lead to an uncertainty of 10% in AOD retrievals.

8.0 Future scope

- The current algorithm will be extended to derive AOD at other spectral wavelengths also.
- Cloud contamination in AOD retrievals at the edges of the clouds may be improved by developing a better cloud mask based on spectral analysis.
- In the current version of the algorithm, the vegetation index is used to know the surface type for surface characterization from visible bands; however, pseudo-albedo may also be a potential variable for the same purpose.
- A similar algorithm can be adapted for OCM-3 on-board upcoming OceanSat-3.
- Knowing AOD, the aerosol correction on level-1 data can be performed for generating surface reflectance and various land products such as surface NDVI.
- Since OCM-2 AOD retrieval is at a very high spatial resolution of 0.7 km, therefore these can be used for atmospheric correction of AWIFS data which will make AWIFS data more useful for agriculture and other land-use applications.
- In the current version, the aerosol model is taken from the work done by Levy et al, 2007 about one decade ago based on global in-situ data from AERONET. However, there is a need for reanalysis/updating of aerosol types over different parts of the world, especially over countries like India with complex atmosphere. This will improve the aerosol retrieval accuracy and will also help in establishing the fine-mode fraction as a quantitative indicator instead of the qualitative indicator for anthropogenic aerosol sources.
- This product is expected to cater inputs for radiative effects of aerosols and air-quality monitoring.

9.0 Discussion

In the present document, we introduced a new algorithm for deriving aerosol properties over land from OCM-2 Level 1B spectral radiance. The beta version of the OCM-2 aerosol product generated using this algorithm is operational from 17 December 2020. Unlike other algorithms, this method does not need SWIR channel observation, moreover, it does not assume near Infrared channels

transparent to aerosols. In fact, in addition to visible channels, it uses aerosol information contained in near Infrared channels also. The OCM-2 aerosol algorithm is tested subjectively as well as on several test datasets. The results are evaluated at co-located AERONET sites. In its provisional validation, OCM-2 AOD retrievals perform well. On average nearly 70% of AOD retrievals found within an uncertainty envelope of 20% with a correlation coefficient $r = 0.83$. Retrievals of fine mode fraction are found to agree with a general understanding of aerosol sources in India and to some extent have been seen correlated with an AERONET size distribution, but quantitatively have not been validated and therefore results should not be considered to be quantitative. We note that the validation of fine mode AOD will be done in near future, which will be a product that can be related to the anthropogenic contribution to the total aerosol optical depth. The provisional validation suggests that the operational beta version retrieval is capable of deriving AOD over land within expected uncertainty. However, it is necessary to perform extensive validation exercises including more ground truth sites with more OCM-2 data.

As already discussed in the introductory section the primary objective of developing this algorithm is intended to cater inputs for radiative and air-quality studies over the Indian landmass. However, with this aerosol product, OCM-2 data utilization can be extended to other land applications also, which was to date limited to ocean Colour applications only. Just as part of this discussion and to appreciate the utility of OCM aerosol product for other land applications, we have shown OCM-2 NDVI product derived with and without aerosol correction in figure 9. The drastic improvement apparent in NDVI establishes the possible utility of this AOD product in many other land applications in addition to radiative and air-quality related studies.

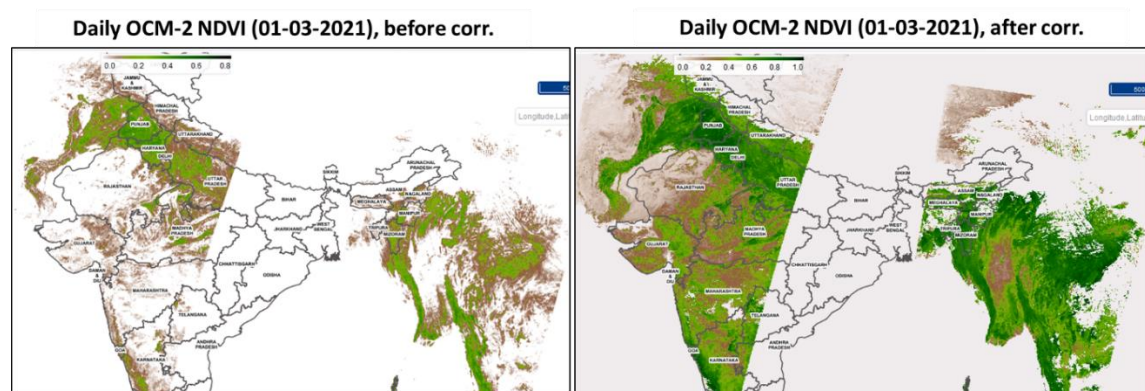


Figure 10. Drastic improvement in OCM-2 derived NDVI after correction for aerosol is apparent in the images shown.

10.0 References

- Charlson, R.J., Langer, J., Rodhe, H., Levoy, C.B. and Warren, S.G., 1991, Perturbation of the northern hemisphere radiative balance by backscattering from anthropogenic sulfate aerosols. *Tellus*, 43AB, pp. 152–163.
- Holben B. N. et al. (1998), AERONET-A federated instrument network and data archive for aerosol characterization, *Remote sensing of environment*, 44 (1), 1-16.
- Haywood, J. and Boucher, O., 2000, Estimates of the direct and indirect radiative forcing due to tropospheric aerosols: a review. *Reviews of Geophysics*, 38, pp. 513–543
- Hansen, J. E., and A. A. Lacis, 1990, Sun and dust versus greenhouse gases: An assessment of their relative roles in global climate change. *Nature*, 346, 713-719.
- Hastings, David A., Paula K. Dunbar, Gerald M. Elphinstone, Mark Bootz, Hiroshi Murakami, Hiroshi Maruyama, Hiroshi Masaharu, Peter Holland, John Payne, Nevin A. Bryant, Thomas L. Logan, J.-P. Muller, Gunter Schreier, and John S. MacDonald, eds., 1999. The Global Land One-kilometer Base Elevation (GLOBE) Digital Elevation Model, Version 1.0. National Oceanic and Atmospheric Administration, National Geophysical Data Center, 325 Broadway, Boulder, Colorado 80305-3328, U.S.A. Digital database on the World Wide Web (URL: <http://www.ngdc.noaa.gov/mgg/topo/globe.html>) and CD-ROMs.
- Hsu, N. C., S. C. Tsay, M. D. King, and J. R. Herman (2004), Aerosol properties over bright-reflecting source regions, *IEEE Trans. Geosci. Remote Sens.*, 42, 557–569.
- Hsu, N. C., S. C. Tsay, M. D. King, and J. R. Herman (2006), Deep blue retrievals of Asian aerosol properties during ACE-Asia, *IEEE Trans. Geosci. Remote Sens.*, 44, 3180–3195.
- Hsu, N. C., M.-J. Jeong, C. Bettenhausen, A. M. Sayer, R. Hansell, C. S. Seftor, J. Huang, and S.-C. Tsay (2013), Enhanced Deep Blue aerosol retrieval algorithm: The second generation, *Geophys. Res. Atmos.*, 118, doi:10.1002/jgrd.50712.
- IPCC (2007), *Climate Change 2007: The Physical Science Basis*, Contribution of Working Group I to the Fourth Assessment Report of the Intergovernmental Panel on Climate Change, edited by S. Solomon et al., Cambridge University Press, Cambridge, United Kingdom and New York, NY, USA.
- Kaufman, Y. J., A. Wald, L. A. Remer, B. C. Gao, R. R. Li, and L. Flynn (1997), The MODIS 2.1- μm channel—Correlation with visible reflectance for use in remote sensing of aerosol, *IEEE. Trans. Geosci. Remote Sens.*, 35(5), 1286–1298.
- Kaufman, Y.J., Tanre, D. and Boucher, O., 2002, A satellite view of aerosols in the climate system. *Nature*, 419, pp. 215–223.
- Levy, R. C., L. A. Remer, S. Mattoo, E. F. Vermote, and Y. J. Kaufman (2007), Second-generation operational algorithm: Retrieval of aerosol properties over land from inversion of Moderate Resolution Imaging Spectroradiometer spectral reflectance, *J. Geophys. Res.*, 112, D13211, doi:10.1029/2006JD007811.
- Platnick, S. and Twomey, S., 1994, Remote sensing the susceptibility of cloud albedo to changes in drop concentration. *Atmospheric Research*, 34, pp. 85–98.

Mishra, M. K. (2018), Retrieval of aerosol optical depth from INSAT-3D imager over Asian landmass and adjoining ocean: Retrieval uncertainty and validation, *J. Geophys. Res. Atmospheres*, 123 (10), 5484-5508.

Richard D. McPeters, P. K. Bhartia, Arlin J. Krueger, Omar Torres, and Jay R. Herman; Earth Probe Total Ozone Mapping Spectrometer (TOMS) Data Products User's Guide; 1998; NASA Technical Publication 1998-206895